

G. Krein · T. C. Peixoto

Femtосcopy of the origin of the nucleon mass

Received:

Abstract We study the prospects of using femtoscopic low-momentum correlation measurements at the Large Hadron Collider to access properties of the J/ψ -nucleon interaction. The QCD multipole expansion in terms of the J/ψ chromopolarizability relates the forward scattering amplitude to a key matrix element to the origin of the nucleon mass problem, the average chromoelectric gluon distribution in the nucleon. We use information on the J/ψ -nucleon interaction provided by lattice QCD simulations and phenomenological models to compute J/ψ -nucleon correlation functions. The computed correlation functions show clear sensitivity to the interaction, in particular to the J/ψ chromopolarizability.

Keywords Quantum chromodynamics · Trace anomaly · Proton mass · Femtосcopy · Heavy-ion collisions

1 Introduction

What is the origin of the mass of protons and neutrons (nucleons) and, therefore, most of the universe’s visible matter? Computer simulations of quantum chromodynamics (QCD) have given an answer to the question, namely: the mass comes mostly from the gluons and the nearly massless quarks. Yet, we are still unsatisfied and want more; we want to understand, to quote Wilczek [1]: “How did it happen?”. With this mindset, an ever-growing effort is underway to find that kind of answer, both theoretically [2, 3] and experimentally [4, 5, 6]. The present work adds to this effort. We study the prospects of using femtосcopy in high-energy proton-proton and heavy-ion collisions for learning about the origin of the nucleon mass.

Femtосcopy [7] is a technique that makes it possible to obtain spatio-temporal information on particle production sources at the femtometer scale. Two-hadron momentum correlation functions carry such information [8, 9]. These correlation functions, remarkably, also carry information on low-energy hadron-hadron forces as final-state effects [10, 11]. Relevant to the origin of the mass problem is the correlation function of a heavy quarkonium (such as J/ψ , η_c , Υ , η_b) and a nucleon, for it gives direct access to the quarkonium-nucleon forward scattering amplitude. The QCD multipole expansion relates this amplitude

G. Krein
Instituto de Física Teórica, Universidade Estadual Paulista, Rua Dr. Bento Teobaldo Ferraz, 271 - Bloco II,
01140-070 São Paulo, SP, Brazil.

T. C. Peixoto
Instituto de Física Teórica, Universidade Estadual Paulista Rua Dr. Bento Teobaldo Ferraz, 271 - Bloco II,
01140-070 São Paulo, SP, Brazil.

and
Instituto Federal de Educação, Ciência e Tecnologia de Sergipe, Rodovia Juscelino Kubitschek, s/n,
49680-000 Nossa Senhora da Glória, SE, Brazil

G. Krein [Corresponding author]
E-mail: gastao.krein@unesp.br

to a key matrix element to the mass problem: the average chromoelectric gluon distribution in the nucleon [12, 13, 14, 15, 16, 17, 18, 19, 20, 21, 22]. It is key to the problem because it relates to the trace of the QCD energy-momentum tensor in the nucleon, which defines the nucleon mass [23, 24].

The quarkonium-nucleon scattering amplitude is also accessible with J/ψ and Υ electro- and photo-production experiments [5]. However, the kinematics of the production process forbids direct access to the forward amplitude. In femtoscopy there are no such kinematics constraints. In addition, the two-particle correlation functions are measurable, in principle, down to zero relative momentum. Exemplar of femtoscopy's capabilities are the hyperon-proton and hyperon-hyperon correlation measurements in heavy-ion (AA), proton-ion (pA) and proton-proton (pp) collisions, ongoing for the last 15 years [25, 26, 27, 28, 29, 30, 31, 32, 33]. Closer to our interest in this paper is the recent feasibility study [34] of the ϕ -proton system using data from pp collisions collected by LHC's ALICE detector. In this and the envisioned quarkonium-nucleon case, the theoretical interpretation of the measurements profits from the absence of the Coulomb interaction and quantum-statistics, features that allow us to link a correlation signal to a strong-interaction effect. Experimentally, however, the situation is not as clear-cut as in theory. Complications arise due to non-femtoscopic correlations, momentum resolution, and other experimental issues, which are always present in an experiment. Such effects need to be accounted for to extract the genuine strong-interaction correlation. In addition, knowledge of the particle source emission form and size are important issues for the theoretical interpretation of the data. Notwithstanding experimental issues, the subject's relevance and successes with the hyperon-proton system and preliminary results on the ϕ -proton system motivate our prospective study. We hope our results will motivate experimental studies as well.

We focus on the J/ψ -nucleon ($J/\psi N$) system, having in mind experiments at the LHC. The motivation for preferring J/ψ over the other heavy quarkonia is twofold. First, J/ψ production yields and weak decay rates are relatively high—the branching ratios of decays to e^+e^- and $\mu^+\mu^-$ is of the order of 6% each. Second, there is some theoretical knowledge on the $J/\psi N$ system from lattice QCD studies [35, 36, 37, 38, 39, 40, 41, 42, 43]. These studies revealed an attractive and not very strong interaction. One lattice study [44] found a bound $\eta_c N$ state with 20 MeV binding, a binding energy much larger than phenomenological expectations [22, 45]. For our femtoscopic study, we use the lattice results of Refs. [35, 36, 37], which provide values for the S -wave scattering length a_0 and effective range r_0 parameters, and of Ref. [38] which gives in addition an S -wave $J/\psi N$ potential extracted with the HALQCD method. These lattice results were obtained either with quenched gluon configurations [35, 37] or large pion masses [36, 38] and, therefore, require extrapolation to the physical mass. A recent study [46] performed such an extrapolation with an effective field theory (EFT) specially set up for studying the low-energy the quarkonium-nucleon interaction. The EFT, dubbed QNEFT, obtained expressions for a_0 and r_0 at leading order (LO) and next-to-leading order (NLO) in the pion mass. The extrapolated values preserve the overall qualitative picture of a weakly attractive interaction. The QNEFT also predicts a model-independent van der Waals type of potential of range $1/2m_\pi \simeq 0.7$ fm, with a strength controlled by the J/ψ chromopolarizability. We note that the $J/\psi N$ system can have spin 1/2 or spin 3/2. The early lattice results of Refs. [35, 36, 37, 38] found no significant hyperfine splitting in a_0 and r_0 . Therefore, the QNEFT extrapolations should be considered as spin-1/2 and spin-3/2 averages. Interestingly, a recent lattice study [41] within the HALQCD method, but with larger lattice volumes and a relativistic heavy quark action for the charm quark, found a somewhat sizable hyperfine splitting, $a_0^{1/2} \simeq 1.7a_0^{3/2}$.

Further knowledge on the $J/\psi N$ interaction comes from phenomenological models. We consider two models, those of Refs. [47, 48]. Both models address the interaction of a charmonium with a nucleon within the hadro-charmonium picture [49]. In this picture, a charmonium interacts as a compact object within the volume of a light hadron. The model of Ref. [47] treats the nucleon as a spherical finite well. This is a very simple but insightful model, as it can be solved analytically. The model of Ref. [48] uses the chiral soliton quark model (χ QSM) of Ref. [50]. The model uses the QCD trace anomaly [51, 52, 53, 54, 55] to obtain an effective $J/\psi N$ potential in terms of the gluon energy-momentum density inside a nucleon calculated with the χ QSM.

We use the knowledge on the $J/\psi N$ system from lattice QCD simulations, extrapolated to the physical pion mass with the QNEFT [46], and from the phenomenological models of Refs. [47, 48] to make predictions for the $J/\psi N$ correlation function. In the next section we review the basics of femtoscopy. We discuss limits for which the correlation function can be linked directly to the scattering amplitude and how this allows us to link the correlation function to the average chromoelectric gluon distribution in the nucleon. In Section 3 we present predictions for the $J/\psi N$ correlation function. We study the dependence of the correlation function on source emission size and on parameters of the interaction. Section 4 presents a summary of our work.

2 Correlation function and scattering amplitude

The observable of interest in femtoscopy is a two-hadron correlation function $C(\mathbf{p}_1, \mathbf{p}_2)$ of measured hadron momenta \mathbf{p}_1 and \mathbf{p}_2 [8,9]. The extraction of the experimental correlation function involves computing the ratio of two yields, $A(k)/B(k)$, where $k = |\mathbf{k}|$ with $\mathbf{k} = \mathbf{p}_1 = -\mathbf{p}_2$, the relative momentum in the center of mass of the pair¹. $A(k)$ is the coincidence yield (or signal distribution), formed by pairs with a given k produced in the same collision event, and $B(k)$ is the uncorrelated yield (or background distribution), formed by pairs with the same k but collected from different collision events. Corrections for non-femtoscopic correlations in $A(k)$ not accounted for in $B(k)$, and other experimental effects, are taken into account by a multiplicative factor $\xi(k)$, so that $C(k) = \xi(k) \times A(k)/B(k)$. The theoretical interpretation of the experimental correlation function is usually based on the Koonin-Pratt formula [10,56]:

$$C(k) = \xi(k) \frac{A(k)}{B(k)} = \int d^3r S_{12}(\mathbf{r}) |\psi(\mathbf{k}, \mathbf{r})|^2. \quad (1)$$

Here $\psi(\mathbf{k}, \mathbf{r})$ is the relative wave function of the pair and $S_{12}(\mathbf{r})$ a static emission source, a pair's relative distance distribution in the pair frame. Refs. [8,9,57,58] address in depth the validity of the assumptions and approximations behind Eq. (1).

The current knowledge of the quarkonium-nucleon interaction lets us assume that it affects only the wave function's S -wave component. Therefore, separating from $\psi(\mathbf{k}, \mathbf{r})$ the $l = 0$ component, $\psi_0(k, r)$, which contains the effects of the strong interaction, we can write $\psi(\mathbf{k}, \mathbf{r})$ as

$$\psi(\mathbf{k}, \mathbf{r}) = e^{i\mathbf{k}\cdot\mathbf{r}} + \psi_0(k, r) - j_0(kr), \quad (2)$$

where $j_0(kr)$ is the $l = 0$ spherical Bessel function, the S -wave component of the non-interacting wave function. Taking a one-parameter Gaussian form for the emission source, $S_{12}(\mathbf{r}) = (4\pi R^2)^{-3/2} \exp(-r^2/4R^2)$, the Koonin-Pratt formula can be written as

$$C(k) = 1 + \frac{4\pi}{(4\pi R^2)^{3/2}} \int_0^\infty dr r^2 e^{-r^2/4R^2} [|\psi_0(k, r)|^2 - |j_0(kr)|^2]. \quad (3)$$

The Gaussian form is a common choice as it simplifies the analysis [59, 60, 61, 62], but it represents an experimental issue, as we discuss in the next section.

Two length scales in $C(k)$ are important for extracting properties of the interaction: the emission source radius R and the two-particle interaction effective range. When these lengths are of comparable size, most of the emitted particles are under the influence of the interaction. Therefore, one needs the pair wave function $\psi_0(k, r)$ in the entire range $0 \leq r \leq \infty$ of integration in Eq. (3). One can use either the Schrödinger equation or the Lippmann-Schwinger equation to obtain $\psi_0(k, r)$; the latter is well suited for treating nonlocal potentials and coupled channels [61, 62]. We deal with local $J/\psi N$ potentials in this paper and use the Schrödinger equation to obtain $\psi_0(k, r)$.

On the other hand, for R much larger than the effective range of the interaction, most of the emitted pairs are not under the influence of the interaction. Then, one can replace $\psi_0(k, r)$ with its asymptotic form

$$\psi_0^{asy}(k, r) = \frac{\sin(kr + \delta_0)}{kr} = e^{-i\delta_0} \left[j_0(kr) + f_0(k) \frac{e^{ikr}}{r} \right] \quad \text{with} \quad f_0(k) = \frac{e^{i\delta_0} \sin \delta_0}{k}, \quad (4)$$

where $f_0(k)$ is the scattering amplitude and δ_0 the phase shift. However, use of $\psi_0^{asy}(k, r)$ in place of $\psi_0(k, r)$ in Eq. (3) for all values of r incurs in error for pairs emitted from within the range of the interaction. One way to account for this error uses [11] effective range theory [63] to evaluate the correction $|\psi_0(k, r) - \psi_0^{asy}(k, r)|^2$ for $r \simeq 0$. Using $\psi_0^{asy}(k, r)$ in place of $\psi_0(k, r)$ in Eq. (3) and including the short-range correction, one obtains for $C(k)$ [11]:

$$C(k) = 1 + \frac{|f_0(k)|^2}{2R^2} \left(1 - \frac{r_0}{2\sqrt{\pi R}} \right) + \frac{2\text{Re} f_0(k)}{\sqrt{\pi R}} F_1(2kR) - \frac{\text{Im} f_0(k)}{R} F_2(2kR), \quad (5)$$

¹ The total momentum is $\mathbf{P} = \mathbf{p}_1 + \mathbf{p}_2$ and the relative momentum is $\mathbf{k} = (m_2 \mathbf{p}_1 - m_1 \mathbf{p}_2)/(m_1 + m_2)$, where m_1, m_2 are the particles' masses. In the center of mass frame, $\mathbf{P} = 0$ and $\mathbf{p}_1 = -\mathbf{p}_2$; hence, the relative momentum is $\mathbf{k} = \mathbf{p}_1 = -\mathbf{p}_2$.

where r_0 the effective range parameter that appears in the effective range expansion (ERE) of $f_0(k)$:

$$f_0(k) = \frac{1}{k \cot \delta_0 - ik} \xrightarrow{k \approx 0} \frac{1}{-\frac{1}{a_0} + \frac{1}{2} r_0 k^2 - ik}, \quad (6)$$

and a_0 is the scattering length, and

$$F_1(x) = \frac{1}{x} \int_0^x dt e^{t-x}, \quad F_2(x) = \frac{1}{x} \left(1 - e^{-x^2}\right). \quad (7)$$

The short-range correction is the term $r_0/2\sqrt{\pi R}$ in Eq. (5); taking $r_0 = 0$ in that equation amounts to replacing $\psi_0(k, r)$ by $\psi_0^{asy}(k, r)$ everywhere in Eq. (3). Of course, to make sense, the correction must be small. Eq. (5) is known as the Lednicky-Lyuboshits (LL) formula. For small values of k , one can use the ERE for $f_0(k)$ and then Eq. (5) becomes universal, in the sense that it depends only on a_0 , r_0 , and R ; no further knowledge is required to compute the correlation function.

If the LL formula is applicable, $C(k)$ at small k gives direct access to the matrix element of the average chromoelectric gluon distribution in the nucleon, $\langle N | (g\mathbf{E}^a) \cdot (g\mathbf{E}^a) | N \rangle \equiv \langle (g\mathbf{E})^2 \rangle_N$, where $\mathbf{E}^a, a = 1, \dots, 8$, is the chromoelectric gluon field, g the strong coupling constant, and $|N\rangle$ the nucleon state. The average $\langle (g\mathbf{E})^2 \rangle_N$ appears in the low energy $J/\psi N$ forward scattering amplitude within the QCD multipole expansion framework, in that the heavy quarkonium behaves like a small color dipole interacting with soft gluon fields of the nucleon [12, 13, 16, 20, 21, 22]. For an S -wave dominating interaction, as it seems to be the case for $J/\psi N$, the forward amplitude at small k is real and given by $f_{\text{forw}}(k) = f_0(k) \simeq -a_0$ [14, 20, 21], with

$$a_0 = \frac{\mu}{4\pi} \alpha_{J/\psi} \langle (g\mathbf{E})^2 \rangle_N, \quad (8)$$

where μ is the $J/\psi N$ reduced mass, $\alpha_{J/\psi}$ the J/ψ chromopolarizability, with $\langle (g\mathbf{E})^2 \rangle_N$ evaluated with the nucleon at rest. Therefore, if the value of $\alpha_{J/\psi}$ is known, one can obtain $\langle (g\mathbf{E})^2 \rangle_N$ from the a_0 extracted from the measured $C(k)$ via the LL formula. Unfortunately, at present $\alpha_{J/\psi}$ is not well constrained by data; as such, while the situation persists, there will be an associated uncertainty in the extraction of $\langle (g\mathbf{E})^2 \rangle_N$. We note that this difficulty is not restricted to femtoscopy; any experiment attempting to extract $\langle (g\mathbf{E})^2 \rangle_N$ from the scattering length via Eq. (8), as for example J/ψ electro- and photo-production experiments [5], share with femtoscopy this difficulty.

If the LL formula is not applicable, the link between the measured $C(k)$ and $\langle (g\mathbf{E})^2 \rangle_N$ is more indirect, as one needs a model for the interaction to extract the scattering length from the experimental $C(k)$. The $\Sigma^+ \Sigma^+$ interaction, discussed in Ref. [61], is an example indicating failure of the LL formula (cf. Fig. [5] of that reference), the failure being associated with the large value of the effective range parameter r_0 . In the next section, we show results for $C(k)$ computed with two models for the $J/\psi N$ interaction for which, depending on the value of $\alpha_{J/\psi}$, r_0 is large.

To conclude this section, we note that the connection between $\langle (g\mathbf{E})^2 \rangle_N$ and the trace of the QCD energy-momentum tensor and the nucleon mass comes through the inequality [21]:

$$\langle N | \left[(g\mathbf{E}^a)^2 - (g\mathbf{B}^a)^2 \right] | N \rangle = -\frac{1}{2} \langle N | g^2 G_{\mu\nu}^a G^{a\mu\nu} | N \rangle = \frac{16\pi^2}{9} m_N \leq \langle (g\mathbf{E})^2 \rangle, \quad (9)$$

where \mathbf{B}^a is the chromomagnetic field. Here we used the trace-anomaly relationship [51, 52, 53, 54, 55]

$$T_{\mu}^{\mu}(x) = -\frac{9}{32\pi^2} g^2 G_{\mu\nu}^a(x) G^{a\mu\nu}(x), \quad (10)$$

valid in the chiral limit. The last inequality in Eq. (9) follows from the fact that $\langle N | (g\mathbf{B}^a)^2 | N \rangle \geq 0$. The normalization of the nucleon state we use is such that the expectation value of T^{00} is the energy [24, 22]. Away from the chiral limit, Eq. (10) contains the contribution from the quark-mass term of the QCD Lagrangian, whose contribution to m_N seems to be small [22].

3 Numerical results and discussions

Here we present predictions for the $J/\psi N$ correlation function. We use information on the $J/\psi N$ interaction from lattice QCD simulations, extrapolated to the physical pion mass with QNEFT [46], and from the phenomenological models of Refs. [47, 48]. Both QNEFT and the phenomenological models consider spin-1/2 and spin-3/2 degeneracy. The radius R of the assumed one-parameter Gaussian form for the emission source is treated as a free parameter; we present results for $R = 1$ fm and $R = 3$ fm. The lower value of R is thought appropriate for pp collisions, and the highest for pA and AA collisions. These are smaller source sizes as those employed in hyperon-nucleon studies [61, 34, 62]. The use of smaller source sizes is motivated by evidence that emission sources scale with the inverse of the emitted particles masses [9]. We recall that the source in femtoscopy refers to the “region of homogeneity”, the region from which particle pairs with a certain momentum are most likely emitted, which is significantly smaller than the size of the entire source emitting particles [8, 9].

We begin presenting results using the QNEFT-extrapolated lattice information [46] for the $J/\psi N$ interaction. The interaction contains contact terms and a long-range, model independent van der Waals potential:

$$V_{\text{vdW}}(r) = \frac{3g_A^2}{128\pi^2 F^2} \{c_{di}[6 + m_\pi r(2 + m_\pi r)] + c_m m_\pi^2 r^2(1 + m_\pi r)^2\} \frac{e^{-2m_\pi r}}{r^6}, \quad (11)$$

where $g_A = 1.27$ is the nucleon axial charge, $F = 93$ MeV the pion decay constant, and c_{di} and c_m are low-energy constants; c_{di} reflects the hadronization into two pions of the soft-gluon coupling $(E^a)^2$ mediating the interaction between the nucleon and J/ψ , and c_m relates to the light-quark masses. The value of c_{di} can be determined by using the QCD trace anomaly [64]. Explicit expressions for c_{di} and c_m are given in Eq. (5) of Ref. [46]; they also depend on the J/ψ chromopolarizability, $\alpha_{J/\psi}$ (denoted by β in that reference), the only parameter in Eq. (11) not well constrained by experiment. Ref. [46] extracted the value $\alpha_{J/\psi} = 0.24$ GeV $^{-3}$ by fitting $V_{\text{vdW}}(r)$ to the $J/\psi N$ HALQCD potential [38]. Given the uncertainties in the lattice values for a_0 and r_0 [35, 36, 37], the corresponding QNEFT-extrapolated values are -0.71 fm $\leq a_0 \leq -0.35$ fm, and 1.29 fm $\leq r_0 \leq 1.35$ fm. We note that a much smaller value for the scattering length, $a_0 = -0.05$ fm, was obtained in Ref. [46] when identifying the LO term of the QNEFT scattering amplitude with the one in Ref. [20], which uses the multipole expansion for quarkonium interaction. A low value for a_0 was also obtained in an earlier study [65] using QCD sum rules, $a_0 = -0.10$ fm. Smaller values were also extracted from old [66] and recent [67, 68] photoproduction data—it should be noted that the extraction of the scattering length in such experiments rely on assumptions and extrapolations to zero momentum transfer, as kinematics forbids direct access to the forward amplitude.

The values of range of the van der Waals force, $1/2m_\pi$, strength at $r = 1/2m_\pi$, 3 MeV, and the values of a_0 and r_0 , justify use of Eq. (5) to compute $C(k)$ for $R = 1$ and $R = 3$. Since the value of the effective range r_0 does not vary much within the uncertainties, we fix it to $r_0 = 1.3$ fm and present results for the scattering length varying in the range -0.7 fm $\leq a_0 \leq -0.05$ fm. Fig. 1 displays results for $C(k)$ for two values of the source radius, $R = 1$ fm and $R = 3$ fm.

Figure 1 reveals the expected trend about correlation strength and source size, in that stronger correlations happen for smaller sources. From this perspective alone, pp collisions are preferred over collisions with heavy ions, although production yields are higher in the latter. Regarding the predictions of the correlation strengths for the different values of the scattering length a_0 , they are small for $R = 3$ fm for the smallest values of a_0 ; namely $C(0) \simeq 1.04$ for $a_0 = -0.10$ fm, $C(0) \simeq 1.02$ for $a_0 = -0.05$ fm. On the other hand, for $R = 1$, the correlation strengths are comparable to those extracted for the ϕN system in Ref. [34].

Next, we present results for $C(k)$ computed with scattering wave functions obtained with the Schrödinger equation for the potentials of Refs. [47] and [48]. The first uses a spherical finite well of radius R_N , given in Eq. (4) of Ref. [47]:

$$V(r) = \begin{cases} -\frac{2\pi}{3} \left(\frac{\alpha_{J/\psi}}{R_N^3}\right) m_N & \text{for } r < R_N \\ 0 & \text{for } r > R_N \end{cases}. \quad (12)$$

The second potential is Eq. (11) of Ref. [48]:

$$V(r) = -\alpha_{J/\psi} \frac{4\pi^2}{b} \left(\frac{g^2}{g_s^2}\right) [v\rho_E(r) - 3p(r)], \quad (13)$$

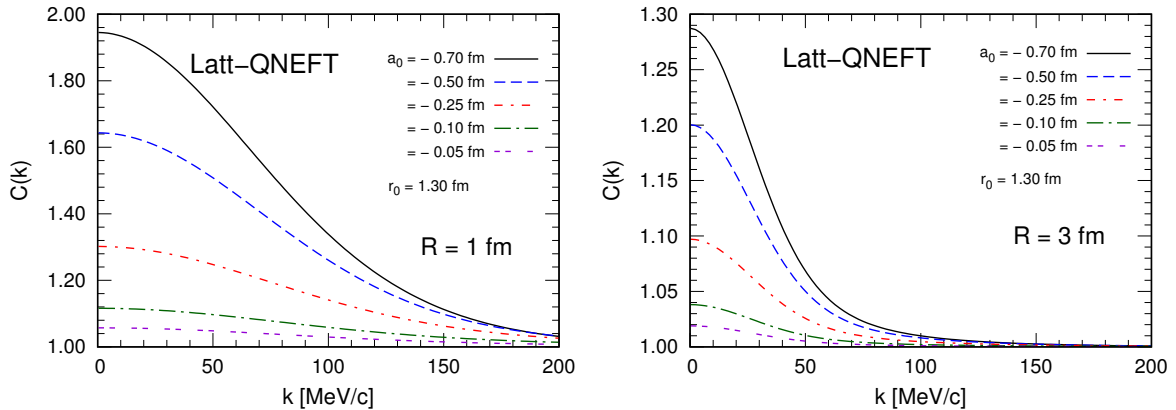


Fig. 1 $J/\psi N$ correlation function computed with Eq. (5) for two values of the source radius R . The a_0 and r_0 values are from lattice QCD simulations [35,36,37,38] extrapolated to the physical pion mass with QNEFT [46].

with $b = (11N_c - 3N_f)/3 = 27/3$ and $g^2/g_s^2 = 1$ (adequate values for J/ψ) and $v = 1.5$. The energy density $\rho_E(r)$ and pressure $p(r)$, given in terms of matrix elements of $T^{00}(x)$ and $T_{\mu}^{\mu}(x)$ in the nucleon state, are computed with the χ QSM in Ref. [50]—we scanned their profiles from Fig. 1 of this reference. In both potentials, only $\alpha_{J/\psi}$ is not well constrained by theory and experiment. Therefore, we present results for $C(k)$ for four values of $\alpha_{J/\psi}$, covering a wide range of values commonly used in the literature, namely: $\alpha_{J/\psi} = 2 \text{ GeV}^{-3}$ [20, 21], 1.60 GeV^{-3} [69], 0.54 GeV^{-3} [65], 0.24 GeV^{-3} [46]. We set the well radius to $R_N = 1 \text{ fm}$, as the results for $C(k)$ with $R = 3 \text{ fm}$ follow the trend shown in Fig. 1.

Table 1 lists the scattering length and effective range parameters extracted from the wave functions. One sees that the a_0 values corresponding to the different $\alpha_{J/\psi}$, for both potentials, are in close correspondence to those used in Fig. 1. Table 1 also reveals the well known fact that when $|a_0|$ is much smaller than the actual range of the potential R_{range} , r_0 can be very different from R_{range} . In this case, use of the ERE for f_0 in the Lednicky model becomes problematic [61].

Table 1 Scattering length and effective range parameters (in fm) corresponding to the finite well with $R_N = 1 \text{ fm}$ and χ SQM potentials, Eqs. (12) and (13), for several values of $\alpha_{J/\psi}$ (in GeV^{-3}).

$\alpha_{J/\psi}$	Finite well		χ SQM	
	a_0	r_0	a_0	r_0
2.00	-0.68	1.59	-0.42	1.86
1.60	-0.47	1.86	-0.30	2.25
0.54	-0.12	4.50	-0.08	6.00
0.24	-0.05	9.46	-0.03	13.05

Figure 2 displays the results for $C(k)$ using the wave functions corresponding to the two potentials. The results for the finite well are very similar to those in Fig. 1. This is not surprising given the fact already mentioned regarding the extracted values of a_0 . The $C(k)$ values for the χ SQM are a little smaller than those for the finite well because the a_0 values are a little smaller for the former.

Given the results in Figs. 1 and 2, one sees that if the $J/\psi N$ interaction turns out to be very weak, to extract information from femtoscopic measurements will be very challenging. As already mentioned, there will always be experimental errors related to source size, momentum resolution, etc that will not allow to resolve weak correlations. In concrete terms, there seems to be room for optimism if the value of the chromopolarizability $\alpha_{J/\psi}$ turns out to be above 0.24 GeV^{-3} .

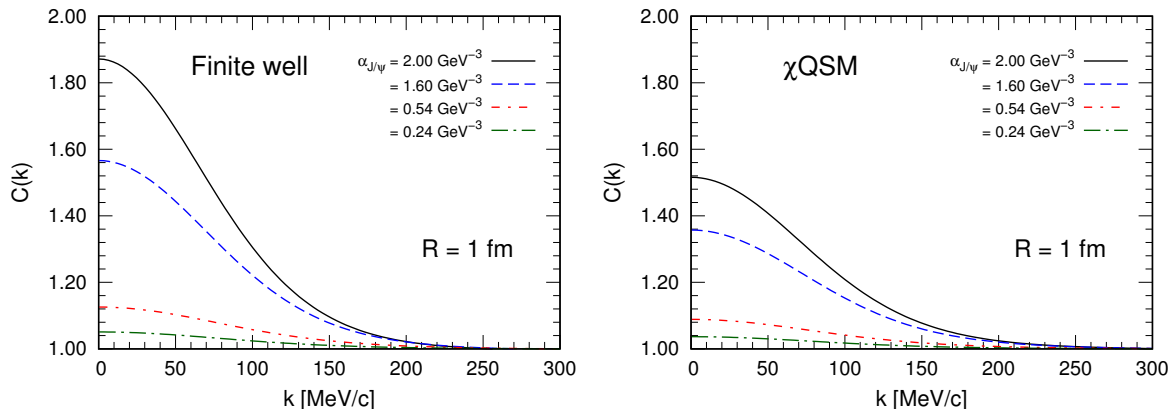


Fig. 2 $J/\psi N$ correlation function calculated with pair wave functions $\psi_0(k, r)$ computed with the Schrödinger equation for the entire range $0 \leq r \leq \infty$ of the integrand of Eq. (3). The $\psi_0(k, r)$ correspond to the potentials in Eqs. (12) and (13).

To conclude, we note that none of these potentials form bound states. A potential well as in Eq. (12) with $R_N = 1$ holds an S -wave bound state when $\alpha_{J/\psi} > 4.4 \text{ GeV}^{-3}$, a value twice as large as the largest value commonly practiced in the literature. The situation is different in the case of a nucleus. Even when the $J/\psi N$ interaction is too weak to bind the two hadrons, nuclear many-body effects play an important role. Of particular importance are the effects of the nuclear mean fields on sub-threshold DD -states [22, 70, 71, 72].

4 Conclusions and perspectives

We studied the prospects of using femtoscopy in high-energy proton-proton and heavy-ion collisions for learning about the low-momentum J/ψ -nucleon interaction. Femtosopic correlation measurements offer the opportunity to access information on low-energy hadron-hadron forces inaccessible by other means. Within the QCD multipole expansion framework, the forward J/ψ -nucleon scattering amplitude is given in terms of the J/ψ chromopolarizability and a key matrix element to the origin of mass problem, the average chromoelectric gluon distribution in the nucleon, which in turn relates to the nucleon mass via the QCD trace anomaly.

Although we focused our study on the J/ψ -nucleon system, femtosopic measurements can also be performed for other heavy quarkonia. Our choice of the J/ψ was motivated by two main facts: the relatively high J/ψ production yields and weak decay rates; and the theoretical information available from lattice QCD simulations and phenomenological models. We made use of this information to compute $J/\psi N$ correlation functions. The available information points towards a relatively short-ranged, weakly attractive interaction. These features of the interaction, together with the QCD multipole expansion framework, lead to a direct relationship between the correlation function at small momenta and the average chromoelectric gluon distribution in the nucleon when using the Lednicky-Lyuboshits (LL) model. Away from the LL model, the link between the chromoelectric gluon distribution in the nucleon and the femtosopic momentum correlation function is less direct. Although one would still have access to information on the interaction, e.g. on scattering parameters, the theoretical interpretation of the data would be more subtle. In any case, the strength of the correlation depends on the J/ψ chromoelectric polarizability, $\alpha_{J/\psi}$, a J/ψ property. This quantity, however, is poorly constrained by experiment. If its value turns out to be $\alpha_{J/\psi} > 0.24 \text{ GeV}^{-3}$, our model calculations indicate a good likelihood for a femtosopic extraction of the average chromoelectric gluon distribution in the nucleon; or else, one will have to find other ways to get it.

We have not addressed experimental issues that can impact the extraction of a low-momentum J/ψ -nucleon correlation function. As already mentioned, nontrivial issues include source form and size, momentum resolution, and non-femtosopic correlations. Notwithstanding these issues, we hope the positive prospects of our theoretical study motivate an experimental study as well.

Acknowledgements Enlightening and useful discussions with Johann Haidenbauer are gratefully acknowledged. G.K was partially supported by: Conselho Nacional de Desenvolvimento Científico e Tecnológico - CNPq, Grants No. Grant. nos.

309262/2019-4, 464898/2014-5 (INCT Física Nuclear e Aplicações), Fundação de Amparo à Pesquisa do Estado de São Paulo - FAPESP, Grant No. 2013/01907-0. T.C.P was supported by a scholarship from Conselho Nacional de Desenvolvimento Científico e Tecnológico - CNPq.

References

1. F. Wilczek, *The lightness of being: Mass, ether, and the unification of forces* (Basic Books, 2008)
2. C.D. Roberts, *Few Body Syst.* **58**(1), 5 (2017). DOI 10.1007/s00601-016-1168-z
3. C.D. Roberts, S.M. Schmidt, arXiv:2006.08782 [hep-ph] (2020)
4. G. Baym (Chair), *An Assessment of U.S.-Based Electron-Ion Collider Science* (The National Academies Press, 2018). DOI 10.17226/25171
5. Z.E. Meziani, S. Joosten, in *Probing Nucleons and Nuclei in High Energy Collisions: Dedicated to the Physics of the Electron Ion Collider* (2020), pp. 234–237. DOI 10.1142/9789811214950\0048
6. X. Chen, F.K. Guo, C.D. Roberts, R. Wang, *Few Body Syst.* **61**(4), 43 (2020). DOI 10.1007/s00601-020-01574-0
7. R. Lednicky, V. Lyuboshits, in *CORINNE 90 - International Workshop on Particle Correlations and Interferometry in Nuclear Collisions* (1990). DOI 10.1142/1178
8. U.W. Heinz, B.V. Jacak, *Ann. Rev. Nucl. Part. Sci.* **49**, 529 (1999). DOI 10.1146/annurev.nucl.49.1.529
9. M.A. Lisa, S. Pratt, R. Soltz, U. Wiedemann, *Ann. Rev. Nucl. Part. Sci.* **55**, 357 (2005). DOI 10.1146/annurev.nucl.55.090704.151533
10. S. Koonin, *Phys. Lett. B* **70**, 43 (1977). DOI 10.1016/0370-2693(77)90340-9
11. R. Lednicky, V. Lyuboshits, *Sov. J. Nucl. Phys.* **35**, 770 (1982)
12. M.E. Peskin, *Nucl. Phys. B* **156**, 365 (1979). DOI 10.1016/0550-3213(79)90199-8
13. G. Bhanot, M.E. Peskin, *Nucl. Phys. B* **156**, 391 (1979). DOI 10.1016/0550-3213(79)90200-1
14. A. Kaidalov, P. Volkovitsky, *Phys. Rev. Lett.* **69**, 3155 (1992). DOI 10.1103/PhysRevLett.69.3155
15. M.E. Luke, A.V. Manohar, M.J. Savage, *Phys. Lett. B* **288**, 355 (1992). DOI 10.1016/0370-2693(92)91114-0
16. D. Kharzeev, *Proc. Int. Sch. Phys. Fermi* **130**, 105 (1996). DOI 10.3254/978-1-61499-215-8-105
17. G.F. de Teramond, R. Espinoza, M. Ortega-Rodriguez, *Phys. Rev. D* **58**, 034012 (1998). DOI 10.1103/PhysRevD.58.034012
18. S.J. Brodsky, G.A. Miller, *Phys. Lett. B* **412**, 125 (1997). DOI 10.1016/S0370-2693(97)01045-9
19. S.H. Lee, C. Ko, *Phys. Rev. C* **67**, 038202 (2003). DOI 10.1103/PhysRevC.67.038202
20. A. Sibirtsev, M. Voloshin, *Phys. Rev. D* **71**, 076005 (2005). DOI 10.1103/PhysRevD.71.076005
21. M. Voloshin, *Prog. Part. Nucl. Phys.* **61**, 455 (2008). DOI 10.1016/j.pnnp.2008.02.001
22. G. Krein, A. Thomas, K. Tushima, *Prog. Part. Nucl. Phys.* **100**, 161 (2018). DOI 10.1016/j.pnnp.2018.02.001
23. M. Shifman, A. Vainshtein, V. Zakharov, *Physics Letters B* **78**(4), 443 (1978). DOI 10.1016/0370-2693(78)90481-1
24. J.F. Donoghue, in *Physics with Light Mesons and on πN Physics*, ed. by W. Gibbs, B. Nefkens (1987)
25. J. Adams, et al., *Phys. Rev. C* **74**, 064906 (2006). DOI 10.1103/PhysRevC.74.064906
26. G. Agakishiev, et al., *Phys. Rev. C* **82**, 021901 (2010). DOI 10.1103/PhysRevC.82.021901
27. L. Adamczyk, et al., *Phys. Rev. Lett.* **114**(2), 022301 (2015). DOI 10.1103/PhysRevLett.114.022301
28. J. Adamczewski-Musch, et al., *Phys. Rev. C* **94**(2), 025201 (2016). DOI 10.1103/PhysRevC.94.025201
29. J. Adam, et al., *Phys. Lett. B* **790**, 490 (2019). DOI 10.1016/j.physletb.2019.01.055
30. S. Acharya, et al., *Phys. Rev. C* **99**(2), 024001 (2019). DOI 10.1103/PhysRevC.99.024001
31. S. Acharya, et al., *Phys. Lett. B* **805**, 135419 (2020). DOI 10.1016/j.physletb.2020.135419
32. S. Acharya, et al., *Phys. Rev. Lett.* **123**(11), 112002 (2019). DOI 10.1103/PhysRevLett.123.112002
33. S. Acharya, et al., *Phys. Lett. B* **797**, 134822 (2019). DOI 10.1016/j.physletb.2019.134822
34. E. Chizali, First measurement of the ϕ -proton correlation function with ALICE in pp collisions at $\sqrt{s} = 13$ TeV. Bachelorarbeit, Technische Universität München, München, Germany (2019)
35. K. Yokokawa, S. Sasaki, T. Hatsuda, A. Hayashigaki, *Phys. Rev. D* **74**, 034504 (2006). DOI 10.1103/PhysRevD.74.034504
36. L. Liu, H.W. Lin, K. Orginos, *PoS LATTICE2008*, 112 (2008). DOI 10.22323/1.066.0112
37. T. Kawanai, S. Sasaki, *PoS LATTICE2010*, 156 (2010). DOI 10.22323/1.105.0156
38. T. Kawanai, S. Sasaki, *Phys. Rev. D* **82**, 091501 (2010). DOI 10.1103/PhysRevD.82.091501
39. T. Kawanai, S. Sasaki, *AIP Conf. Proc.* **1388**(1), 640 (2011). DOI 10.1063/1.3647474
40. M. Aliberti, G.S. Bali, S. Collins, F. Knechtli, G. Moir, W. Söldner, *Phys. Rev. D* **95**(7), 074501 (2017). DOI 10.1103/PhysRevD.95.074501
41. T. Sugiura, Y. Ikeda, N. Ishii, *EPJ Web Conf.* **175**, 05011 (2018). DOI 10.1051/epjconf/201817505011
42. U. Skerbis, S. Prelovsek, *Phys. Rev. D* **99**(9), 094505 (2019). DOI 10.1103/PhysRevD.99.094505
43. T. Sugiura, Y. Ikeda, N. Ishii, *PoS LATTICE2018*, 093 (2019). DOI 10.22323/1.334.0093
44. S. Beane, E. Chang, S. Cohen, W. Detmold, H.W. Lin, K. Orginos, A. Parreño, M. Savage, *Phys. Rev. D* **91**(11), 114503 (2015). DOI 10.1103/PhysRevD.91.114503
45. A. Hosaka, T. Hyodo, K. Sudoh, Y. Yamaguchi, S. Yasui, *Prog. Part. Nucl. Phys.* **96**, 88 (2017). DOI 10.1016/j.pnnp.2017.04.003
46. J. Tarrús Castellà, G. Krein, *Phys. Rev. D* **98**(1), 014029 (2018). DOI 10.1103/PhysRevD.98.014029
47. J. Ferretti, E. Santopinto, M. Naeem Anwar, M. Bedolla, *Phys. Lett. B* **789**, 562 (2019). DOI 10.1016/j.physletb.2018.09.047
48. M.I. Eides, V.Y. Petrov, M.V. Polyakov, *Eur. Phys. J. C* **78**(1), 36 (2018). DOI 10.1140/epjc/s10052-018-5530-9
49. S. Dubynskiy, M. Voloshin, *Phys. Lett. B* **666**, 344 (2008). DOI 10.1016/j.physletb.2008.07.086
50. K. Goetze, J. Grabis, J. Ossmann, M. Polyakov, P. Schweitzer, A. Silva, D. Urbano, *Phys. Rev. D* **75**, 094021 (2007). DOI 10.1103/PhysRevD.75.094021
51. M.S. Chanowitz, J.R. Ellis, *Phys. Lett. B* **40**, 397 (1972). DOI 10.1016/0370-2693(72)90829-5
52. R. Crewther, *Phys. Rev. Lett.* **28**, 1421 (1972). DOI 10.1103/PhysRevLett.28.1421

-
53. M.S. Chanowitz, J.R. Ellis, *Phys. Rev. D* **7**, 2490 (1973). DOI 10.1103/PhysRevD.7.2490
 54. D.Z. Freedman, I.J. Muzinich, E.J. Weinberg, *Annals Phys.* **87**, 95 (1974). DOI 10.1016/0003-4916(74)90448-5
 55. J.C. Collins, A. Duncan, S.D. Joglekar, *Phys. Rev. D* **16**, 438 (1977). DOI 10.1103/PhysRevD.16.438
 56. S. Pratt, *Phys. Rev. Lett.* **53**, 1219 (1984). DOI 10.1103/PhysRevLett.53.1219
 57. W. Bauer, C. Gelbke, S. Pratt, *Ann. Rev. Nucl. Part. Sci.* **42**, 77 (1992). DOI 10.1146/annurev.ns.42.120192.000453
 58. D. Anchishkin, U.W. Heinz, P. Renk, *Phys. Rev. C* **57**, 1428 (1998). DOI 10.1103/PhysRevC.57.1428
 59. A. Ohnishi, K. Morita, K. Miyahara, T. Hyodo, *Nucl. Phys. A* **954**, 294 (2016). DOI 10.1016/j.nuclphysa.2016.05.010
 60. K. Morita, A. Ohnishi, F. Etminan, T. Hatsuda, *Phys. Rev. C* **94**(3), 031901 (2016). DOI 10.1103/PhysRevC.94.031901. [Erratum: *Phys.Rev.C* 100, 069902 (2019)]
 61. J. Haidenbauer, *Nucl. Phys. A* **981**, 1 (2019). DOI 10.1016/j.nuclphysa.2018.10.090
 62. J. Haidenbauer, G. Krein, T. Peixoto, *Eur. Phys. J. A* **56**(7), 184 (2020). DOI 10.1140/epja/s10050-020-00190-0
 63. H. Bethe, *Phys. Rev.* **76**, 38 (1949). DOI 10.1103/PhysRev.76.38
 64. N. Brambilla, G. Krein, J. Tarrús Castellà, A. Vairo, *Phys. Rev. D* **93**(5), 054002 (2016). DOI 10.1103/PhysRevD.93.054002
 65. A. Hayashigaki, *Prog. Theor. Phys.* **101**, 923 (1999). DOI 10.1143/PTP.101.923
 66. O. Gryniuk, M. Vanderhaeghen, *Phys. Rev. D* **94**(7), 074001 (2016). DOI 10.1103/PhysRevD.94.074001
 67. I. Strakovsky, D. Epifanov, L. Pentchev, *Phys. Rev. C* **101**(4), 042201 (2020). DOI 10.1103/PhysRevC.101.042201
 68. L. Pentchev, I.I. Strakovsky, arXiv:2009.04502 [hep-ph] (2020)
 69. M.V. Polyakov, P. Schweitzer, *Phys. Rev. D* **98**(3), 034030 (2018). DOI 10.1103/PhysRevD.98.034030
 70. K. Tsushima, D. Lu, G. Krein, A. Thomas, *Phys. Rev. C* **83**, 065208 (2011). DOI 10.1103/PhysRevC.83.065208
 71. G. Krein, A. Thomas, K. Tsushima, *Phys. Lett. B* **697**, 136 (2011). DOI 10.1016/j.physletb.2011.01.037
 72. G. Krein, *J. Phys. Conf. Ser.* **422**, 012012 (2013). DOI 10.1088/1742-6596/422/1/012012